



Title	ECR Plasma in a High Power Millimeter-Wave Beam (Report III) : Difference in Plasma Property by Axial and Radial Launches(Welding Physics, Process & Instrument)
Author(s)	Arata, Yoshiaki; Miyake, Shoji; Kishimoto, Hiroaki et al.
Citation	Transactions of JWRI. 1986, 15(2), p. 213-219
Version Type	VoR
URL	<a href="https://doi.org/10.18910/12670">https://doi.org/10.18910/12670</a>
rights	
Note	

*The University of Osaka Institutional Knowledge Archive : OUKA*

<https://ir.library.osaka-u.ac.jp/>

The University of Osaka

# ECR Plasma in a High Power Millimeter-Wave Beam (Report III)

## — Difference in Plasma Property by Axial and Radial Launches —

Yoshiaki ARATA \*, Shoji MIYAKE \*\*, Hiroaki KISHIMOTO \*\*\*, Nobuyuki ABE \*\*\*\*  
and Yoshinobu KAWAI \*\*\*\*\*

### Abstract

*In the production and heating of an ECR plasma in a simple mirror field by a high power millimeter-wave beam, it was found that the difference in the launching direction of the beam to a mirror field gave a remarkable influence to the plasma property. Radial distribution of the hot electron component was affected by the beam expansion in the plasma chamber and the position of the fundamental and the 2nd harmonic resonance zones. In the axial launch a bell-shape radial distribution of the plasma was typically observed, and in the radial launch a ring-shape distribution was obtained. In the former the fundamental resonance zone and in the latter the 2nd harmonic zone played an important role in the plasma production and heating. It was also clarified that in the build-up phase of the plasma, a dense fully ionized plasma with an electron density reaching to the cut-off frequency of the wave was easily obtained. A preliminary result of gas puffing during the power input indicated a comfortable effect of increasing the electron density and suppressing an unstable oscillation.*

**KEY WORDS:** (Electron Cyclotron Frequency) (ECR Plasma) (Millimeter-Wave Beam) (Gyrotron) (Wave Mode)  
(2nd Harmonic Heating)

### 1. Introduction

In Report II<sup>1)</sup> time variation of electron density was studied by changing various external parameters. In the duration of 100 ms of the power input from the Gyrotron, the line integrated density increased rapidly to a maximum value within 1 ms or so after the power input, after which it decreased to a quasi-steady value accompanying the prompt decrease of the neutral particles by the pumping action of the plasma. In addition, in the afterglow phase the secondary ionization was observed by the residual hot electrons. The maximum value of  $n_e L$ , however, was not clarified in detail. Meanwhile an example of the X-ray radiation from the plasma measured by the pure-Ge semiconductor detector was shown in Report I<sup>2)</sup>. But this data was found to be doubtful because of severe shielding problem of the scattered radiation. In many researches on the ECR plasma production and heating in a simple mirror field so far, comprehensive surveys have not been performed on the following points; 1) difference in the role of fundamental (1st) and 2nd harmonic resonance heating, 2) comparison of the difference in the plasma properties by the wave launching direction to the plasma, 3) spatial distribution of the hot electron plasma, 4) maximum attainable density to a value of the cut-off of the millimeter-wave, 5) energy distribution of the plasma electrons, 6) effect of the difference in

the configuration of the mirror field, 7) wall effect.

We have tried to make a comprehensive study on these points except 6) and 7). In Report II only the data in the radial launch of the wave was described. In this paper data in the axial launch of the wave are reported as well as the radial injection. Since the estimation of the electron density  $n_e$  from the line integrated density  $n_e L$  is influenced by the radial distribution of the plasma, it is important to know the spatial distribution of various informations, such as visible, VUV or soft X-ray emission from the plasma. Among them we have performed to measure the soft X-ray emission in the energy range of 0.1 – 2 keV with a gas-flow proportional counter by the energy dispersive detection of the X-ray and this easy-to-handle detector could make us know the radial distribution of the soft X-ray in different operating conditions. As for the measurement of X-ray in the high energy range over 10 keV, we have used a Si (Li) and/or a pure-Ge detector. But at present they give us not so important information on the variation of the plasma properties with external parameters. Indeed, to solve the problem 5), measurement by these three detectors should be closely correlated and it will be reported in the forthcoming paper.

In this paper mainly differences in the plasma property by the axial and the radial launches of the wave are reported from the data obtained by using a gas-flow

\* Received on Nov. 7, 1986

\*\* Professor

\*\*\* Associate Professor

\*\*\*\* Graduate Student

\*\*\*\*\* Research Instructor

Transactions of JWRI is published by Welding Research Institute of Osaka University, Ibaraki, Osaka 567, Japan

proportional counter. Also is shown a preliminary result on the effect of the gas puffing to improve the decrease of the electron density during the power input.

## 2. Experimental Apparatus

In this report the mirror ratio  $MR$  is fixed to be 2. While two methods of the wave injection to the plasma were tried; the radial and the axial launch. In launching the millimeter-wave to the mirror field in the axial direction, a myter-bend was used to connect the waveguide directly to the vacuum chamber from the one end.

For the measurement of soft X-ray from the plasma, a Si (Li) semiconductor detector is used in the energy range of 1 – 30 keV, and below 2 keV a gas-flow type proportional counter (Model 04, Manson) is used. The cylindrical counter has a fine anode wire tightened on its axis. The window of the counter is made from a quite thin VYNS film spread on the fine mesh of 60% transmission. The counter gas is P-10 which consists of 90% argon which serves for absorption of the low energy photons and 10% methane for the stable operation of the counter at a low gas pressure and a high anode voltage. The gas pressure in the counter is fixed to 200 Torr and the anode high voltage is set around 1 kV. The overall detection efficiency is calculated to be approximately 40% for the soft X-ray energy range of 0.2- 2 keV. On account of a very poor sensitivity above 3 keV, it is not so severe to measure the soft X-ray emission of 0.1 – 2 keV without thick shielding over the counter against the scattered high energy X-ray radiation. In fact we could successfully obtain the radial distribution of the soft X-ray emission from the plasma.

A preliminary experiment on the gas puffing in the plasma production is also carried out. The fast-acting valve is controlled by the rapid opening of a piezoelectric plate. The influx is regulated by the applied voltage and its pulse length to the plate.

## 3. Results and Discussion

### 3.1 Build-up phase in the plasma production

The line integrated electron density  $n_eL$  is measured with a 4 mm microwave interferometer in the radial direction, where  $L$  is a typical plasma dimension. It has been reported in Report II that during the power input of the wave to the plasma,  $n_eL$  reaches to a maximum value rapidly after the start of the discharge, but it is decreased to a quasi-steady value within 5 to 10 ms. As the maximum value is obtained within 1 ms or so from the start of the discharge, it is not so easy to follow the variation of fringe patterns in this phase. The maximum fringe num-

bers was estimated by obtaining the data at various pulse durations within 10 ms and by counting the fringe numbers for each duration in their afterglow phases. Figure 1 shows the dependence of the maximum  $n_eL$  on the millimeter-wave power  $P_\mu$  in the axial and the radial launches of the wave. When the gas pressure is low with a value of  $5.1 \times 10^{-3}$  Pa, the maximum  $n_eL$  amounts to about  $9 \times 10^{13} \text{ cm}^{-2}$  at about 20 kW, but it saturates at a higher power. When we assume a radial plasma dimension of about 20 cm, the maximum  $n_e$  is approximately  $5 \times 10^{12} \text{ cm}^{-3}$  in this case and the plasma is considered to be in a fully ionized state. We can see that the more the gas pressure, the stronger the increase of the maximum  $n_eL$  with the input power. When the millimeter-wave is launched in the radial direction, a value of  $n_eL$  higher than  $5 \times 10^{14} \text{ cm}^{-2}$  is obtained at  $P_\mu \simeq 50 \text{ kW}$  and  $p_0 = 3.6 \times 10^{-2} \text{ Pa}$ . Due to the strong absorption and the refraction effect of the 4 mm microwave of the interferometer, it was difficult to measure a higher  $n_eL$  than this value. When we assume  $L = 20 \text{ cm}$ ,

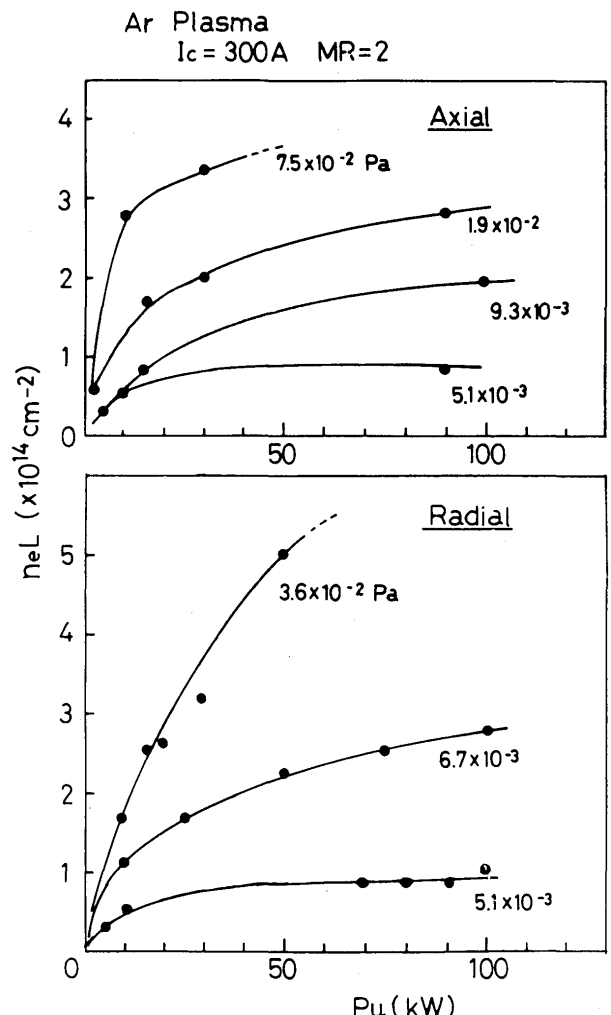


Fig. 1 Dependence of the maximum  $n_eL$  to be obtained in the build-up phase of the plasma on the input power of the millimeter-wave.

$n_e$  reaches to  $2.5 \times 10^{13} \text{ cm}^{-3}$  which is about a half of the cut-off density of the Gyrotron 5 mm wave, and this again confirms the production of a fully ionized plasma. While the production of a plasma by axially launching the wave seems to be not so efficient. But when the radial dimension of the plasma varies drastically by the difference in the launching direction, it is not correct to give a further comment only from this result.

We may consider, nevertheless, that a high density plasma reaching to the cut-off density is obtained in the early time of the injection below 1 ms by a high power input, although it is rapidly pumped away in the axial direction accompanying a strong decrease of the residual gas pressure.

### 3.2 Effect of gas puffing

In a long pulse operation with a constant gas flow rate through a needle valve, it was usually found out that the diamagnetic flux starts to increase from the time when the electron density has fallen down to a quasi-steady value. The intensity of the visible emission has shown a similar variation with that of the electron density. To recover a rapid decrease of the electron density, a preliminary experiment was performed to use a fast-acting gas valve, by which rapid supply of the ionizing gas would

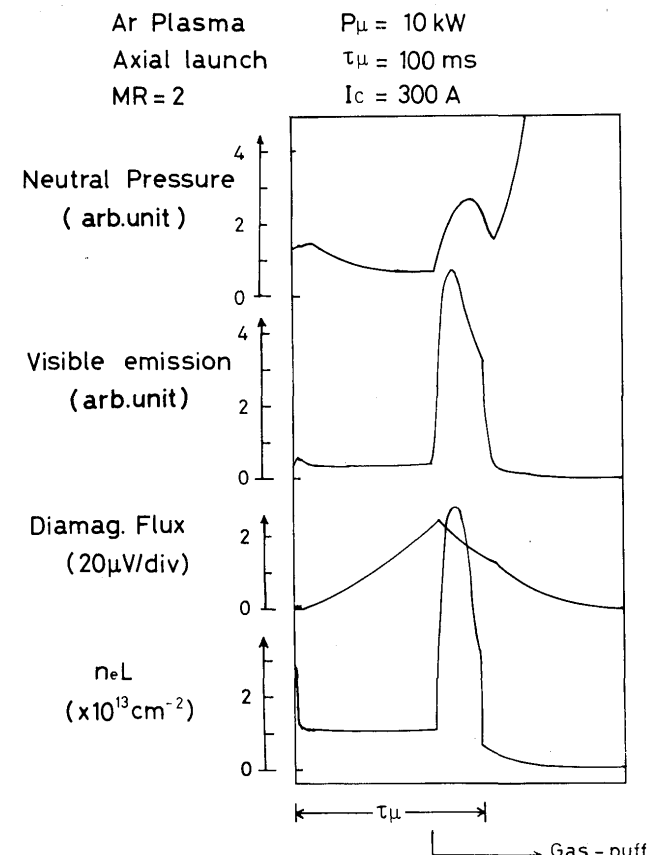


Fig. 2 Trace of various signals at  $P_\mu = 10 \text{ kW}$  with gas puffing.

produce a higher electron density.

Figure 2 shows a typical example of the time variation of various signals in the case of gas puffing during the pulse input. The pulse width  $\tau_\mu$  of the wave beam is fixed to be 100 ms and the input power is 10 kW. The gas-puff starts from  $t = 70 \text{ ms}$ . The line density  $n_eL$  shows a prompt increase after this time, but it again begins to decrease until the end of the wave input. The visible emission shows a very high intensity after the puff, but it also decreases again as well as  $n_eL$ . On the other hand, the diamagnetic flux begins to decrease by the gas-puff. These data imply that increment of the electron density is assured by the gas-puff, but it also induces cooling of the plasma as is usually the case. In this data the duration of the gas-puff is longer than 30 ms. Variation of the neutral gas pressure was detected by the nude-type ionization gauge as shown in the figure. It is remarked that, in spite of the gas-puff, the neutral pressure does not continue to increase during the power input. This result indicates that the pumping action of the plasma out of the mirror region is still so strong inducing again the rapid lowering of the residual neutral gas in the plasma.

The gas-puff is able to stabilize some unstable oscillations as well as to increase  $n_e$ . Figure 3 shows similar data as in Fig. 2. As shown in (b), when the gas-puff is

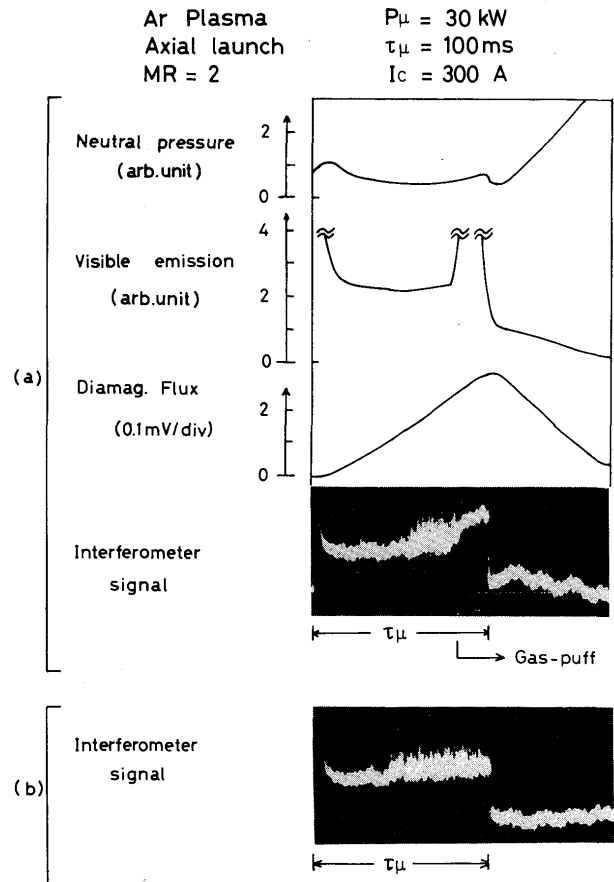


Fig. 3 Trace of various signals at  $P_\mu = 30 \text{ kW}$  with gas puffing.

not used, the fringe pattern of the interferometer includes a high frequency spiking signal after  $t \geq 40$  ms. When a small gas-puff is applied at  $t \geq 80$  ms as shown in (a), this noise in the fringe pattern vanishes and a stable mode is achieved with a slight increase of the electron density and no decrease in the diamagnetic signal. The neutral pressure shows quite a little increase for  $t \leq 100$  ms. It is interesting to note that the visible emission is increased remarkably by the gas-puff. It will reflect the increase of the excited state particles in accordance with the density enhancement.

By this preliminary experiment, we could not obtain an overall control of the gas-puff to obtain a quasi-steady high density state without a sharp decrease in  $n_e$  in the early time of the power input and with a constant intensity of the diamagnetic signals. The more refined experiments are needed and their results will be reported in a subsequent paper.

### 3.3 Soft X-ray measurement

In general, Bremsstrahlung X-ray radiation from a plasma reflects the property of the hot electron component. However it has been remarked recently that an ECR plasma in a mirror field would include several components in the electron temperature<sup>3)</sup> and/or would have an energy distribution<sup>4)</sup> different from the Maxwellian one, by which it is doubtful to define the hot electron temperature by the measurement of X-ray spectrum within a small definite energy range. While, detailed studies on the soft X-ray emission in the energy range of 0.1 – 10 keV has been carried only by us, and when the application of an ECR plasma to the soft X-ray source is taken into consideration, measurement of the soft X-ray emission in this energy range is very important.

Figures 4 and 5 show some examples of the soft X-ray spectra below 2 keV. They are the raw data and must be corrected by the detector efficiency. From the calibration of the detector by the exposure from a standard soft X-ray source (Model 2, Manson), efficiency of the detector was found to be about 40% except for the extremely low energy photons below 100 eV in agreement with the calculated value.

In Fig. 4 the time-integrated data are given for various powers of the millimeter-wave. The pulse duration of the beam  $\tau_\mu$  is 1 ms in this case. These spectra indicate that the larger the input power, the higher the average electron energy. As described in 3.1, in the build-up stage of the plasma, the electron density  $n_e$  does not increase in proportion to the beam power in a low gas pressure. But in this data a large power input is found to be effective to heat electrons. The tail of the spectrum above 1 keV becomes conspicuous with the power increase. Here we remark that the proportional counter is set near the

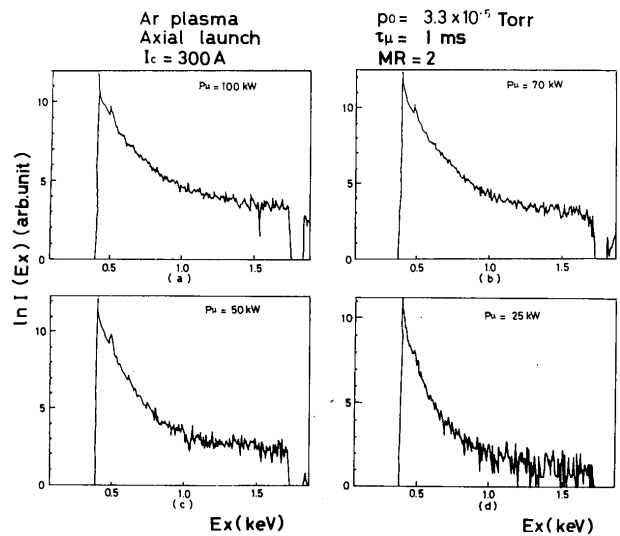


Fig. 4 Soft X-ray spectrum from the plasma obtained by the proportional counter for various input powers.

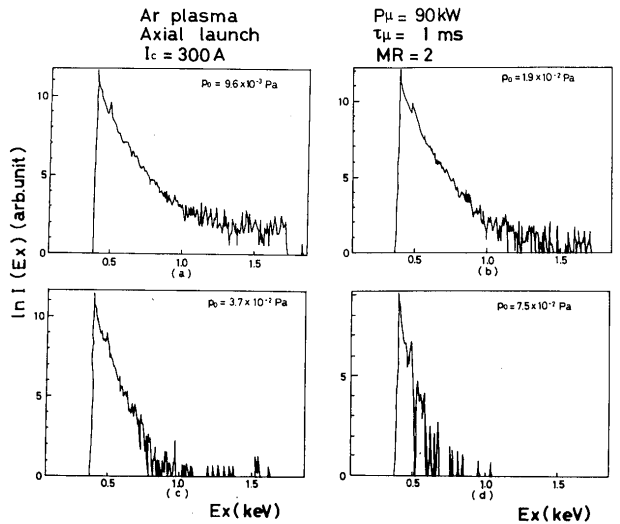


Fig. 5 Soft X-ray spectrum from the plasma obtained by the proportional counter for different gas pressures.

plasma chamber and connected by the pipe including a lead collimator. The detector housing is made of brass and is not shielded against the scattered high energy X-ray. So that the observed tail might include Compton's continuum of the scattered radiation. The energy resolution of the proportional counter is not so good as a Si (Li) or a pure-Ge semiconductor detector. In addition, it still has a small sensitivity to the tail of Ar-K $\alpha$  3 keV radiation. These problems must be carefully corrected when we want to obtain a quantitative estimation on the energy spectra.

In Fig. 5 are shown similar spectra at different gas pressures. At a high pressure of  $7.5 \times 10^{-2}$  Pa, the tail of the spectrum disappears and a constant slope can be easily drawn in the low energy continuum. A calculation of the spectrum to be obtained by this detector was carried out for the continuum emission from the plasma

electrons with a Maxwellian distribution, taking into account the energy resolution of the detector. It has indicated that, for a single Maxwellian distribution, a logarithmic spectrum consists of a quasi-straight line bent halfway at about 400 eV. In high pressures such as 3.7 and  $7.5 \times 10^{-2}$  Pa the average energy of hot electrons is low and a high energy tail is not observed. In this case, definition of a single hot electron temperature  $T_e$  is possible in this energy region, when we can neglect the contribution of line emissions which will come from multiply charged ions in a charge state more than 10. By setting the proportional counter in the adjacent room screened by the concrete wall, we could correctly avoid to be confused by the influence of the scattered radiation to the measured data. By this arrangement spectra similar to the calculated one could be obtained not only in Ar plasma but also in H<sub>2</sub> plasma in which no line emission is included in this energy region. So that we demonstrate that when we apply a proportional counter with careful calibration procedures, it is possible to estimate the electron energy distribution in the range of 0.1 – 2 keV.

### 3.4 Radial distribution of hot electron components

The gas-flow type proportional counter is vertically scanned to estimate the radial distribution of hot electron component. In the measurement, the proportional counter is set near the plasma chamber. In this case continuum spectrum by the Compton's scattering might be included as we have described in 3.3. Count rate of the plasma X-ray continuum, however, was so large that this low level background signal could be neglected when we selected photons below 1 keV.

First we have measured the distribution in the radial launch of the wave. Figure 6 shows an example of the radial distribution of soft X-ray intensity with an energy of 400 eV on the midplane of the plasma column for various values of the coil current  $I_c$ . The Abel inversion of the data is not performed. In the figure the radial position of the 2nd harmonic resonance zone is marked by  $2\omega_{ce}$  on the abscissa. In (a) of the figure, the 2nd harmonic resonance zone is located at  $x = 10$  cm when  $I_c = 300$  A. While we can see that the peak of the intensity appears at  $x = 8$  cm. The same tendency is also shown in (b) and (c). By the Abel transformation of these data, each peak will shift to the outside and will coincide with the position of  $2\omega_{ce}$ . We can demonstrate that a hot electron ring is obtained when the 2nd harmonic resonance point is located at an off-axial position in the radial direction. While in the case of  $I_c = 230$  A, the 2nd harmonic zone lies near the center and the distribution forms a core plasma at the center. It is interesting to note that another peak around  $x = 10$  cm is observed. Indeed this point corresponds to the 3rd harmonic resonance

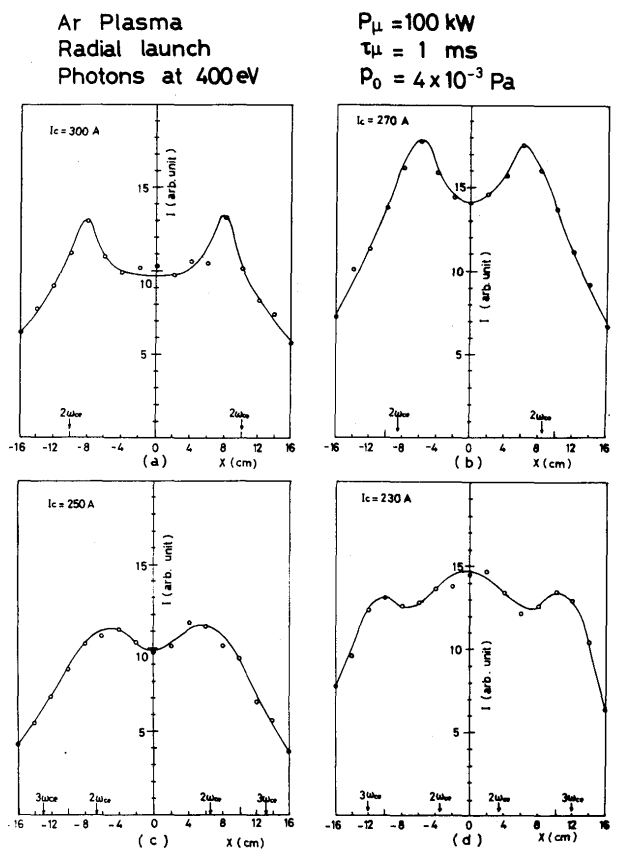


Fig. 6 Lateral distributions of soft X-ray emission with an energy of 400 eV from the plasma in the case of the radial launch of the wave.

zone marked by  $3\omega_{ce}$ .

In the axial launch, on the other hand, the radial distribution was found to be quite different from the ones in Fig. 6. The result is shown in Fig. 7. Although  $P_\mu$  and  $\tau_\mu$  are different from those in Fig. 7. It was certified that the distribution did not differ so much with  $P_\mu$  and  $\tau_\mu$  in the case of the radial launch. In (a) of the figure the distribution shows a strong peak at the center and a small hump near the position of  $2\omega_{ce}$  is also found. While in (b) the hump appears more sharply by the increase in the input power. The intensity at the center is still very strong in contrast to the case of the radial launch found in Fig. 6 (a). It was verified further that when the power input was lowered to 2 kW, the hump at the 2nd harmonic position disappeared.

These results can be explained as follows. In both of radial and axial launches, a cylindrical over-sized waveguide of 63.5 mm in diameter is connected directly to the vacuum chamber through a BeO vacuum window. As the wavelength of the Gyrotron millimeter wave is about 5 mm, the wave can propagate into the chamber with a small divergent angle of about 10°. Figure 8 shows the calculated wave mode pattern injected into a free space from this waveguide. The beam with cylindrical TE<sub>02</sub> mode has two peaks in the distribution of electric field in

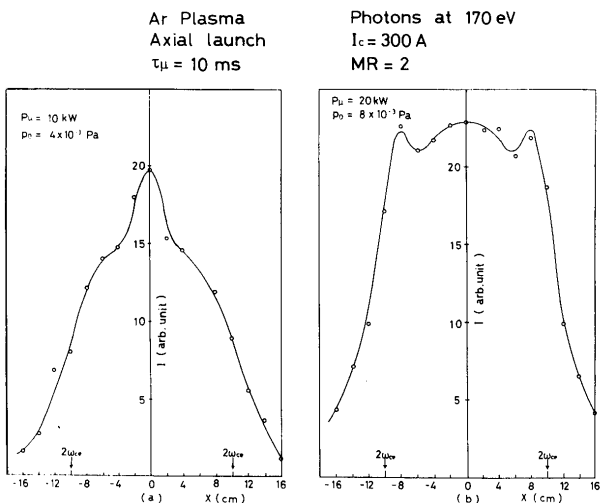


Fig. 7 Lateral distributions of soft X-ray emission with an energy of 400 eV from the plasma in the case of the axial launch of the wave.

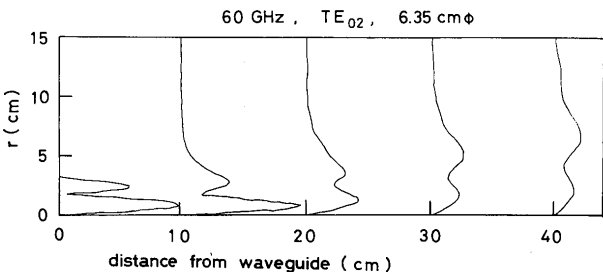


Fig. 8 Calculated mode pattern of the 60 GHz millimeter-wave injected into a free space with  $TE_{02}$  mode from an oversized cylindrical waveguide.

the radial direction. As the dimension of the vacuum chamber is large enough, we may consider that the propagation of the wave in the chamber is similar to that in the free space. In the axial launch, the 2nd harmonic zone at  $I_c = 300$  A exists at  $r = 10$  cm on the midplane and the distance between the midplane and the wave launching position corresponding to the end of the waveguide is about 35 cm in the axial direction. So that from Fig. 8 the wave energy near the 2nd harmonic zone is considered to be weak in comparison with the one at the fundamental resonance position of  $z = 15$  cm on this axis. Thus only at a relatively high power input, heating at the 2nd harmonic zone is observed, and production and heating of the plasma is mainly performed at the fundamental resonance zones. Meanwhile as for the radial launch, the 2nd harmonic resonance zone lies at  $r = 10$  cm on the midplane at  $I_c = 300$  A, and the mirror axis is about 20 cm away in the radial direction from the launching position. Moreover the fundamental resonance zone is located on the plane at  $z = 10$  cm at the same coil current. We may easily assume that the wave beam does not reach directly to the fundamental resonance zone. Rather the production and heating only at the 2nd harmonic resonance zones will be more effective, by which we have obtained a

hollow shape in the distribution in Fig. 6. This result is different from an ECR plasma produced by a microwave radiation of  $f = 2.45$  GHz<sup>5)</sup>. In that case the wavelength is over 10 cm and the wave is considered to be distributed almost uniformly within the vacuum chamber. In the axial launch of the wave effect of the 1st and the 2nd harmonic heating was equally observed even though the input power was as low as 1 kW or so.

Thus a spatially restricted local heating is possible when the wave frequency is high enough for the wave to be injected into a limited area of the resonance zone. We also remark that the distributions shown in Figs. 6 & 7 indicate that the distribution of the electron density  $n_e$  might also vary with the change in the operating conditions. So that to decide  $n_e$  from the line integrated  $n_e L$  by the 4 mm-interferometer needs much care.

#### 4. Conclusion

Pulsed ECR Plasma production and heating in a simple mirror field was studied with a 60 GHz Gyrotron in detail.

In the start-up phase of the plasma production, the millimeter-wave energy was consumed efficiently to produce a dense plasma in a fully ionized state. We found a strong dependence of the electron density on the power input, by which we could easily obtain a very high density state nearly equal to the cut-off density of the wave, although it again rapidly decreased to a quasi-steady value by the strong pumping effect of the plasma, inducing a lowering of the neutral particle density during the power input. This strong decrease of the electron density could be recovered with gas puffing, and it also served to suppress an oscillation induced from the plasma instability. Radial distribution of the hot electron component strongly depended on the launching direction and the divergence of the millimeter-wave beam, which was also correlated with the position of the fundamental and the second harmonic resonance zones. In the axial launch, hot electrons with a core in the plasma center were formed and they were produced mainly by the fundamental resonance heating. In a high power input a ring shape distribution was additionally obtained at the second harmonic zone. While in the radial launch, the fundamental resonance zone was found to contribute little to the formation of the hot components. In this case the 2nd harmonic zone played an important role in obtaining a ring or a bell-shape distribution on the midplane of the plasma column.

#### Acknowledgement

The authors would like to express their gratitude to Prof. Yamamoto and Dr. K. Oda for their interest and

critical comment to this work. They also thank Mr. Wada, Kyoto University for preparing us calculated beam patterns.

#### Reference

- 1) Y. Arata, S. Miyake, N. Abe, H. Kishimoto, Y. Agawa and Y. Kawai: *Trans. JWRI* **14** (1985) 41.
- 2) Y. Arata, S. Miyake, N. Abe, H. Kishimoto, Y. Agawa and Y. Kawai: *Trans. JWRI* **13** (1984) 9.
- 3) M. E. Mauel: *Phys. Fluid* **27** (1984) 2899.
- 4) K. Wiesemann: *Proc. 8th Symp. on ISIAT'84 (Tokyo)*, 59.
- 5) Y. Arata, S. Miyake, H. Kishimoto, Y. Agawa and N. Abe: *Trans. JWRI* **15-2**; this issue.